Available online at www.sciencedirect.com
ScienceDirect
Lithos 97 (2007) 271 – 288
LITHOS
www.elsevier.com/locate/lithos

Origin of high field strength element enrichment in volcanic arcs: Geochemical evidence from the Sulu Arc, southern Philippines

P.R. Castillo *, S.J. Rigby, R.U. Solidum [1]

Scripps Institution of Oceanography, UCSD, La Jolla, CA 92093-0212, USA

Received 7 July 2005; accepted 13 December 2006
Available online 20 December 2006

Abstract

Lavas from the Sulu Arc, southern Philippines, exhibit an enrichment in high field strength elements (HFSE) that represents a departure from the typical volcanic arc geochemical signature. It has been postulated that this relative enrichment arises from metasomatism of mantle wedge peridotites by melts derived from the subducting oceanic lithosphere, through formation of amphibole which subsequently breaks down and enriches the mantle source of parental arc magmas in HFSE. Divergent chemical and isotopic characteristics between Sulu Arc HFSE-enriched lavas and the Sulu Sea crust being subducted—the presumed source of slab-derived melts—render it unlikely, however, that HFSE enrichment arises from the influence of such melts. New geochemical data suggest that the varying degrees of HFSE enrichment in Sulu Arc lavas are instead the result of variable amounts of mixing between enriched and depleted mantle end-components—the sources of South China Sea intraplate lavas and Sulu seafloor basalts, respectively—within a compositionally heterogeneous mantle wedge.

Keywords: High field strength elements (HFSE); Adakites; Sulu Arc; Philippines; Island arc; High-Nb basalts

1. Introduction

A distinctive geochemical feature of subduction zone lavas is a general enrichment in the abundances of some of the incompatible trace elements such as large ion lithophile elements (LILE; e.g. Rb, K, Ba, Sr) and light rare earth elements (LREE; e.g. La, Ce, Nd), but a strong depletion in high field strength elements (HFSE; e.g. Nb, Ta, Zr, Ti, Hf) (e.g., Gill, 1981; Hawkesworth et al., 1991; Woodhead et al., 1993; Pearce et al., 1999). Arc lavas are thus typically characterized by high LILE/HFSE and LREE/HFSE ratios, and by negative anomalies in Nb, Hf, Ta, and sometimes Zr or Ti, on chondrite- or mantle-normalized trace element plots. This relative depletion in HFSE stands in contrast with lavas from other tectonic settings, such as mid-ocean ridge or ocean island basalts (MORB and OIB, respectively), which are characterized by relatively smooth, primitive mantle-normalized trace element patterns.

The typical enrichment of arc lavas in LILE and LREE has been attributed to metasomatism of the sub-arc mantle source by slab-derived fluids enriched in these elements (e.g., Tatsumi et al., 1986; Hawkesworth et al., 1991, 1993; McCulloch and Gamble, 1991; Pearce and Peate, 1995). The origin of the characteristic

* Corresponding author. Tel.: +1 858 5340383; fax: +1 858 8224945.
E-mail address: pcastillo@ucsd.edu (P.R. Castillo).
[1] Now at: Philippine Institute of Volcanology and Seismology, Diliman, Quezon City, Philippines.

0024-4937/$ - see front matter
doi:10.1016/j.lithos.2006.12.012

HFSE depletion is less straightforward, and has been frequently ascribed to the lower solubilities, relative to LILE and LREE, of HFSE in slab-derived fluids (e.g., Tatsumi et al., 1986; Maury et al., 1992; Brenan et al., 1994). Other proposed mechanisms have included prior extraction of HFSE from the mantle due to previous partial melting (e.g., McCulloch and Gamble, 1991; Gamble et al., 1993; Woodhead et al., 1993) and preferential partitioning into solid phases, either into residual phases during magma segregation (Green and Pearson, 1986; Reagan and Gill, 1989; Elliot et al., 1997; Foley et al., 2002; Schmidt et al., 2004) or within the asthenosphere through melt/rock interaction during magma ascent (Kelemen et al., 1990, 1993).

Some volcanic arc mafic lavas exhibit enrichment in HFSE and thus possess low LILE/HFSE and LREE/HFSE ratios, weakly negative or even positive Nb anomalies, and comparatively high TiO_2 contents relative to other arc mafic magmas. Due to their unusually high-Nb concentrations (>20 ppm versus <4 ppm for typical arc lavas) these mafic lavas have been labeled high-Nb basalts (HNB) (Reagan and Gill, 1989; Defant et al., 1991). They have been reported to occur in several modern arc systems, including Panama and Costa Rica (Reagan and Gill, 1989; Defant et al., 1992), the Cascades (Leeman et al., 1990; Defant and Drummond, 1993), Kamchatka (Kepezhinskas et al., 1996), and Baja California (Aguillón-Robles et al., 2001).

Reagan and Gill (1989) proposed that the distinctive geochemistry of the HNB arises from two melting stages, resulting in a mixture of reduced melts undersaturated in rutile and high-degree melts of upwelling mantle. An alternate model is metasomatism of the mantle wedge by melts derived from the subducting basaltic crust, termed “adakites” (Kepezhinskas et al., 1996; Defant and Kepezhinskas, 2001). Adakites and HNB have been found to be closely associated (Leeman et al., 1990; Defant et al., 1992; Defant and Drummond, 1993; Kepezhinskas et al., 1996; Aguillón-Robles et al., 2001). The suggested role of adakite melts in the generation of Nb enrichment in these modern arc systems has also been used to attribute the genesis of Achaean rocks with relative Nb enrichment to a similar process (Wyman et al., 2000; Hollings, 2002).

Sajona et al. (1993, 1994, 1996) reported adakites and mafic lavas with trace element ratios similar to HNB but with lower absolute Nb concentrations (7–16 ppm) from the northeastern segment of the Sulu Arc, southern Philippines (Fig. 1). Consequently, they proposed that the enrichment in Nb in these lavas, which they termed Nb-enriched basalts and basaltic andesites (NEB), is the result of melting of a mantle source that had been previously metasomatized by melts derived from the subducted Sulu Sea basaltic crust. Castillo et al. (2002), however, later reported the presence of both NEB and HNB (up to 48 ppm Nb) in Jolo and Marungas islands in the central segment of the Sulu Arc, and suggested that the geochemical characteristics of Sulu Arc lavas enriched in Nb are best explained by the presence of pockets of a geochemically enriched component within the sub-arc mantle rather than by the influence of slab-derived melts.

The behavior of HFSE in convergent margin magmatism is germane to our understanding of the fate of crustal materials that have been recycled into the mantle through subduction. In this study, we try to constrain the best model for the origin of HFSE enrichment in the Sulu Arc. We analyze new trace element and Sr–Nd–Pb isotopic data for typical NEB and adakites from the northeastern Sulu Arc (Sajona et al., 1993, 1994, 1996) and compare these with those of the NEB and HNB from the central Sulu Arc (Castillo et al., 2002). The broad spectrum of geochemical data for these lavas allows us to investigate in more detail than previous studies the chemical variations within and possible relationships among the different HFSE-enriched lava groups and assess the efficacies of proposed models for the origin of HFSE enrichment at the Sulu convergent margin. We then present the possible implications of our results on the generation of other HFSE-enriched arc lavas.

2. Geological background and samples

Mindanao Island, in the southern Philippines, is bordered by at least three active subduction zones—the Philippine Trench to the east, Cotabato Trench to the southwest and the Sulu–Negros Trench in the northwest (Fig. 1; Hamilton, 1979). The Sulu Trench segment of the Sulu–Negros Trench system marks the location of aseismic subduction of Sulu Sea crust south–southeast beneath Celebes Sea crust, and is associated with the Sulu Arc (Castillo et al., 2002). This arc is defined by a northeast-trending linear chain of small volcanic islands along the boundary between the Sulu and Celebes Seas and by the arc volcanoes on the Zamboanga Peninsula in northwestern Mindanao. The Sulu Sea crust currently being subducted beneath the Sulu Arc originated from a small basin that formed—either as a back-arc basin or a marginal basin analogous to the South China Sea (Rangin and Silver, 1991)—in either the early Miocene (Rangin and Silver, 1991) or the Oligocene (Roeser, 1991). Subduction of Sulu Sea crust first occurred along

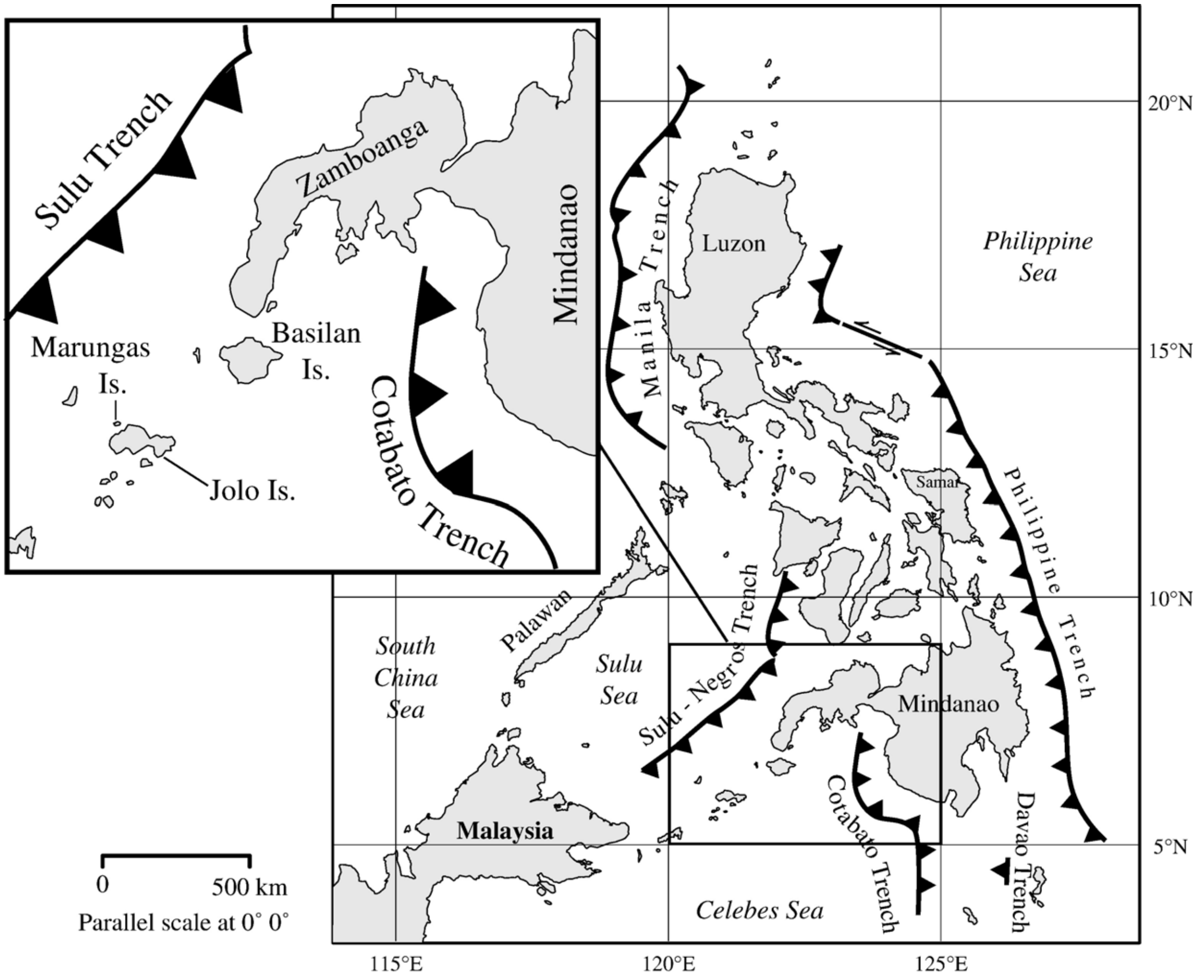

Fig. 1. Generalized tectonic map of the Philippines. Inset shows the Sulu Arc. Northeastern segment samples mentioned in the text are from Zamboanga Peninsula and Basilan Island, whereas central segment samples are from Jolo Island and nearby Marungas Island.

the proto-Sulu Trench in the early–middle Miocene but both subduction and opening of the Sulu Sea halted in the late Miocene, the probable result of the collision between the central Philippines and the Eurasian margin (Pubellier et al., 1991; Rangin and Silver, 1991). After the closure of the Molucca Sea in the Pliocene, subduction resumed along the Sulu Trench (Pubellier et al., 1991). At present, there is a high geothermal gradient—up to 200 °C/km near the northeastern end of the trench—most likely due to the subduction of the extinct Sulu spreading center (Hinz and Block, 1990; Sajona et al., 1996). Zamboanga Peninsula basement rocks include Cretaceous peridotite, metamorphosed continent-derived sediments, Tertiary metavolcanics, and slivers of ophiolitic rock (Pubellier et al., 1991; Apuada et al., 1992; Santos and Pamatian, 1995; Sajona et al., 1996).

Lavas from the northeastern segment of the Sulu Arc, in the central and eastern portions of the Zamboanga Peninsula and in Basilan Island (Fig. 1), termed the Zamboanga Arc by Sajona et al. (1996), vary from basalts and basaltic andesites to dacites and rhyolites. The basalts and basaltic andesites range from aphyric to porphyritic samples with omnipresent olivine phenocrysts. The more differentiated andesites and dacites are porphyritic, containing plagioclase and amphibole phenocrysts set in a fine-grained, glassy matrix. Samples from the Zamboanga Arc were previously analyzed by Sajona et al. (1993, 1996) for their major and trace elements through inductively coupled plasma-atomic emission spectroscopy (ICP-AES) with the exception of Rb, which was done by atomic absorption spectroscopy.

Lavas from the volcanic islands of Jolo and Marungas in the central segment of the Sulu Arc comprise mainly of basalts and basaltic andesites (Castillo et al., 2002). The samples are generally fresh, fine-

Table 1
Major and trace elements and Sr, Nd and Pb isotope composition of representative Sulu Arc lavas

Sample	S-3	S-4	S-7	S-8	S-11	S-12	S-14	P90-35	PH93-38	PH93-39	PH93-10	PH90-17B	PH93-18	P90-20	P90-61	JB-1 ave. measured (n=18)	Standard deviation	Recommended values
Arc segment	Central	Central	Central	Central	Central	Central	Central	NE	NE	NE	NE	NE	NE	NE	NE			
Rock type	prim bas	prim bas	prim bas	prim bas	bas and	bas and	bas and	Mg bas	Mg bas	Mg bas and	CA bas and	lwK bas and	Adakite	Adakite	hiK bas and			
SiO_2 (wt.%)	48.03	47.31	46.81	48.25	53.97	53.54	53.36	50.74	52.90	51.33	55.18	53.34	67.48	64.97	54.96			
TiO_2	1.72	1.84	2.25	2.11	2.05	2.00	1.79	1.66	1.72	1.67	1.32	1.02	0.35	0.38	0.90			
Al_2O_3	15.30	16.12	14.04	13.72	15.68	14.97	15.04	15.42	14.42	15.29	16.79	17.17	17.22	18.08	17.99			
$Fe_2O_3^{total}$	11.70	12.10	13.22	12.51	11.72	11.31	10.24	11.72	11.14	11.28	8.88	9.29	3.35	4.13	7.71			
MgO	8.87	8.90	8.56	8.64	5.00	5.62	5.46	6.85	7.46	7.57	4.93	6.24	1.65	1.58	4.06			
CaO	9.91	9.19	8.96	9.63	7.84	8.31	8.87	9.43	8.55	8.80	7.79	8.68	4.26	5.22	8.23			
Na_2O	2.93	3.48	4.22	2.99	3.23	3.49	3.84	3.04	2.87	3.04	3.56	3.50	4.33	4.16	3.11			
K_2O	0.88	0.63	1.50	1.58	0.24	0.44	1.02	0.49	0.54	0.58	1.04	0.46	1.14	1.25	2.34			
P_2O_5	0.49	0.28	0.27	0.42	0.15	0.20	0.25	0.27	0.24	0.29	0.40	0.16	0.15	0.14	0.56			
Total	99.84	99.84	99.83	99.84	99.88	99.86	99.87	99.61	99.84	99.85	99.87	99.86	99.94	99.91	99.85			
V (ppm)	225	223	159	200	170	157	141	188	190	186	143	166	72	67	235			
Cr	273	311	275	277	198	205	168	250	274	224	135	200	28	41	26			
Co	44	54	54	49	39	40	37	58	44	42	32	39	14	12	25			
Ni	182	195	220	213	128	141	104	190	190	180	82	108	17	21	13			
Rb	13.5	6.9	23.7	38.5	4.1	8.0	15.2	8.0	9.3	10.5	24.5	10.5	22.7	26.0	68.0			
Sr	563	567	414	660	207	278	387	351	298	356	572	375	460	464	950			
Y	21.5	16.3	20.0	25.5	14.4	22.2	23.8	28.0	23.4	26.0	18.80	20.0	9.50	10.0	28.0			
Zr	141	147	153	146	129	128	127	102	128	107	162	70	88	58	185			
Nb	29.9	32.2	47.6	41.0	9.7	9.0	11.1	12.0	25.8	13.8	16.4	4.0	2.6	2.0	7.7			
New analyses:																		
Ba (ppm)	267	303	467	437	62	98	170	109	93	132	254	152	253	254	1073	487	8.52	490
La	21.34	14.29	15.88		4.52	6.04	9.49	9.77	6.93	9.33	23.70	7.53	8.04	6.65	39.69	37.90	0.41	38
Ce	41.61	30.19	29.46		9.89	12.67	18.70	20.47	16.35	20.35	46.56	16.10	16.08	14.71	78.90	67.06	0.53	67
Nd	21.29	13.86	16.09		8.84	10.75	14.33	13.20	12.36	13.54	22.38	10.78	8.06	8.15	35.93	26.91	0.16	27
Sm	4.97	3.46	4.57		3.41	4.19	4.77	3.88	4.18	4.14	4.97	3.06	1.70	1.91	7.35	5.01	0.07	5

Eu	1.69	1.41	1.68		1.37	1.69	1.77	1.43	1.54	1.51	1.67	1.18	0.61	0.68	2.21	1.51	0.03	1.52
Tb	0.74	0.53	0.83		0.69	0.85	0.90	0.70	0.77	0.74	0.69	0.58	0.24	0.28	0.97	0.75	0.01	0.76
Dy	3.99	2.95	4.03		3.26	4.34	4.47	4.01	4.50	4.29	3.68	3.60	1.33	1.59	5.08	4.04	0.07	4
Er	1.93	1.42	1.84		1.53	2.10	2.20	2.09	2.29	2.26	1.80	2.14	0.77	0.91	2.70	2.19	0.04	2.2
Yb	1.53	1.12	1.51		1.24	1.78	1.89	1.65	1.81	1.82	1.47	1.90	0.74	0.86	2.45	2.11	0.04	2.1
Lu	0.22	0.17						0.24	0.26	0.26	0.22	0.28	0.12	0.14	0.36	0.31	0.01	0.31
Hf	3.02	2.90	3.57	3.30	3.13	3.07	3.15	3.01	13.68	2.63	14.09	13.89	2.08	1.95	9.28	3.40	0.20	3.4
Ta	1.70	1.58	2.46	2.29	0.41	0.41	0.66	0.98	3.58	0.67	4.37	2.08	0.20	0.21	1.18	2.70	0.10	2.7
Pb	2.0	3.1	2.1	2.52	1.3	1.4	2.2	0.81	4.91	1.70	2.49	1.91	6.15	6.03	23.12	7.02	0.16	7.1
Th	3.80	3.37	3.63	3.19	0.86	1.16	1.79	1.69	0.66	1.16	5.08	1.25	2.15	1.38	13.01	9.12	0.21	9.2
U	0.88	0.84	0.83	0.85	0.36	0.42	0.64	0.37	1.41	0.43	0.84	0.33	0.49	0.34	2.79	1.64	0.06	1.7
Nb/Ta	17.5	20.4	19.3	17.9	23.3	22.1	16.9	12.2	7.2	20.6	3.8	1.9	13.2	9.4	6.5			
Zr/Hf	46.6	50.9	43.0	44.2	41.3	41.6	40.4	33.9	9.4	40.7	11.5	5.0	42.3	29.8	19.9			
Zr/Sm	28.3	42.6	33.6	37.9	30.5	26.7		26.3	30.7	25.8	32.6	22.9	51.6	30.4	25.2			
$^{86}Sr/^{88}Sr$	*0.703663*		*0.703727*	0.703768	*0.703408*	0.703427	*0.703447*		0.703584	0.703608	0.703598		0.703693		0.705041			
	10		*10*	10	*11*	10	*10*		11	12	12		11		12			
$^{143}Nd/^{144}Nd$	*0.512921*		*0.512919*	0.512924	*0.503066*	0.513039	*0.513009*		0.512965	0.512948	0.512929		0.512946		0.512686			
	9		*7*	13	*7*	13	*9*		8	8	7		8		7			
$^{206}Pb/^{204}Pb$	18.476		18.338	18.335	18.419	18.407	18.407		18.482	18.431	18.390		18.253		18.573			
	2		3	3	4	3	2		3	2	6		2		2			
$^{207}Pb/^{204}Pb$	15.573		15.531	15.540	15.546	15.539	15.556		15.572	15.539	15.587		15.545		15.641			
	2		3	3	4	2	1		2	2	6		1		2			
$^{208}Pb/^{204}Pb$	38.520		38.364	38.401	38.378	38.353	38.391		38.505	38.377	38.494		38.240		38.817			
	4		7	7	9	6	4		6	4	14		3		5			

Note: prim bas = primitive basalt; bas and = basaltic andesite; Mg bas = magnesian basalt; Mg bas and = magnesian basaltic andesite; CA bas and = calk-alkaline basaltic andesite; lwK bas and = low-K basaltic andesite; hiK bas and = high-K basaltic andesite. Major oxides, trace elements and Sr–Nd isotopic ratios previously reported by Sajona et al. (1996) and Castillo et al. (2002) are in italics. The precisions in terms of relative standard deviations for the ICP-AES analyses reported by Sajona et al. (1993, 1996) are ≤2% for major elements except for MnO and P_2O_5, and ≤5% for the trace elements. Those for the XRF analyses reported by Castillo et al. (2002) are <2% for major elements except for Na_2O and Mn (<5%), <5% for Cr, Rb, Sr, V, Y, Zr, and Ni and <8% for Co and Nb. For the new analyses, replicate analyses of the JB-1 standard show trace element precision be ≤2% for Ba and REE except Lu (<4%), <4% for Ta, Pb, Th, and U and 5% for Hf. Recommended JB-1 values are from Govindaraju (1989). Analytical uncertainty for $^{87}Sr/^{86}Sr$ measurements is ±0.000012 and for $^{143}Nd/^{144}Nd$ is ±0.000014; uncertainties for Pb isotopic ratios are approximately ±0.015 for $^{206}Pb/^{204}Pb$ and $^{207}Pb/^{204}Pb$ and ±0.025 for $^{208}Pb/^{204}Pb$. The uncertainties shown are instrument errors, and refer to the last significant digits. Sr isotopic ratios were measured by dynamic multi-collection mode, fractionation-corrected to $^{86}Sr/^{88}Sr=0.1194$ and normalized to $^{87}Sr/^{86}Sr=0.71025$ for NBS 987. Nd isotopic ratios were measured in oxide form and fractionation-corrected to $^{146}NdO/^{144}NdO=0.72225$ ($^{146}Nd/^{144}Nd=0.7219$) and are reported relative to $^{143}Nd/^{144}Nd=0.511850$ for the La Jolla Nd Standard (measured La Jolla Nd values are 0.511860). Pb isotopic ratios were corrected for mass fractionation based on average measured values for NBS 981 using the values of Todt et al. (1996).

grained and aphyric to slightly olivine- and plagioclase-microphyric and were analyzed for major elements by X-ray fluorescence (XRF), trace elements by XRF and Sr and Nd isotopes by thermal ionization mass spectrometry (TIMS) (Castillo et al., 2002).

For this study, representative samples from the northeastern and central segments of the Sulu Arc were analyzed for additional trace elements (i.e., Ba, rare earth elements (REE), Hf, Ta, Pb, Th, and U) by high-resolution inductively coupled mass spectrometry (HR-ICP-MS). Strontium, Nd and Pb isotope ratios of a subset of the northeastern Sulu Arc samples as well as Pb isotope ratios of the central Sulu Arc whole rock samples previously analyzed by Castillo et al. (2002) for Sr and Nd isotopes, were measured through TIMS. All analyses were done at the Scripps Institution of Oceanography using established procedures there (e.g., Lugmair and Galer, 1992; Janney and Castillo, 1996; Castillo and Newhall, 2004). Estimated accuracy and precision of the different analytical methods are described as notes under Table 1.

3. Compositional variation

3.1. Major elements

Lavas from the northeastern segment of the Sulu Arc show significant variation in their major element compositions (Sajona et al., 1993, 1994, 1996). They range from basalt to rhyolite belonging to the low-K tholeiitic to medium-K calc-alkaline lava suites, and include a high-K calc-alkaline basaltic andesite (Fig. 2). Four distinct lava groups were recognized by Sajona et al. (1996): magnesian (6.6–7.6% MgO) basalts and basaltic andesites, calc-alkaline basaltic andesites, low-K basalts and basaltic andesites, and evolved andesites and dacites that display adakitic compositions. From the northeastern segment, we have samples of two magnesian basalts (P90-35, PH93-38; Table 1), a magnesian basaltic andesite (PH93-39), a calc-alkaline basaltic andesite (PH93-10), a low-K basaltic andesite (PH90-17B), two adakites (PH93-18, P90-20), and the lone high-K basaltic andesite (P90-61). Samples analyzed from Jolo and Marungas islands in the central segment of the Sulu Arc have more restricted major element compositions (Fig. 2; Castillo et al., 2002). These samples can be subdivided into two groups, one consisting of primitive (8.0–8.8 wt.% MgO) medium-K calc-alkaline to shoshonitic basalts (46.6–48.7 wt.% SiO_2) while the other is low-K tholeiitic to medium-K calc-alkaline basaltic andesites. The latter group overlaps with the basalts and basaltic andesites from the northeastern segment. The former group, however, is clearly distinct from the northeastern segment lavas and is more akin to the intraplate basalts from the Reed Bank and Scarborough Seamount in the South China Sea (Fig. 2; Tu et al., 1992). From the central segment, we have four samples of the primitive basalts (S-3, S-4, S-7, S-8) and three samples of basaltic andesites (S-11, S-12, S-14; Table 1). Both the northeastern and central sample

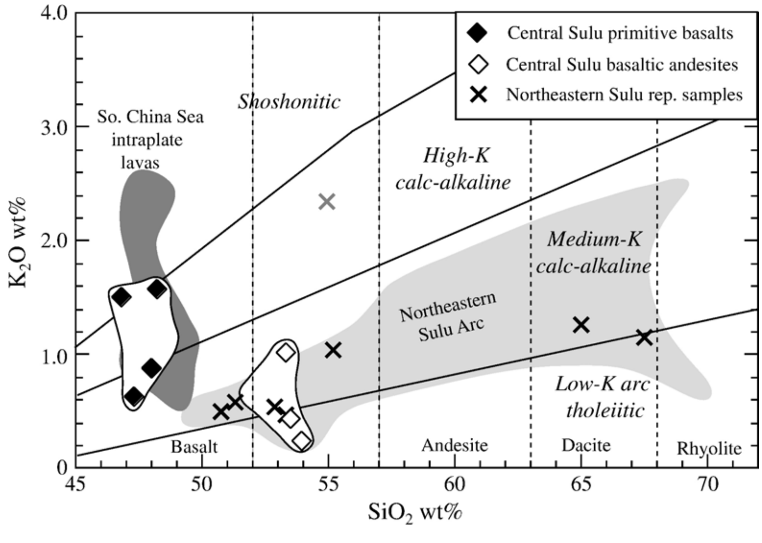

Fig. 2. K_2O versus SiO_2 (wt.%) classification diagram for Sulu samples, modified from Peccerillo and Taylor (1976). Shaded field encompasses full set of analyses of northeastern segment samples by Sajona et al. (1993, 1996), of which representative samples (high-K calc-alkaline andesite is shown in grey) were incorporated into this study. Also shown is the shaded field for South China Sea intraplate basalts from Scarborough and Reed Bank Seamounts (Tu et al., 1992).

groups are of Pliocene–Pleistocene age (Sajona et al., 1996; Castillo et al., 2002).

Despite the large variation in major element composition, all Sulu samples roughly define consistent trends from basalt to adakite on Harker diagrams (Fig. 3; see also, Sajona et al., 1996). Most major elements generally increase (e.g., Al_2O_3, Na_2O) or decrease (e.g., MgO, TiO_2, Fe_2O_3*, CaO) as SiO_2 wt.% increases. However, the basalts and basaltic andesites show a wide range of TiO_2, Al_2O_3, and Na_2O values for a given SiO_2.

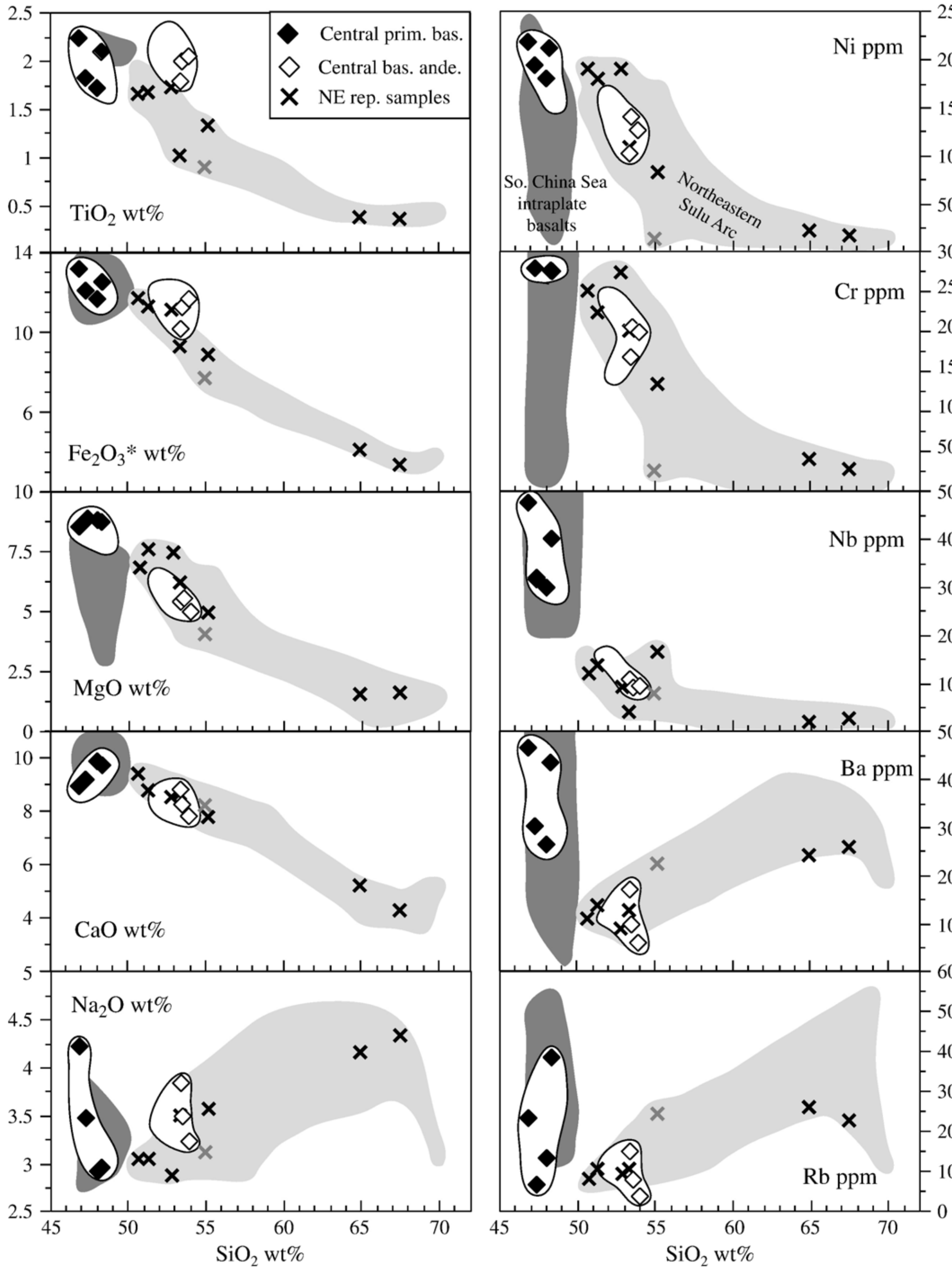

Fig. 3. SiO_2 (wt.%) versus selected major and trace elements for representative Sulu Arc lavas. Symbols as in Fig. 2. Fields for full set of analyses for the central segment HNB and NEB, northeastern segment (Sajona et al., 1993, 1996) and South China Sea intraplate lavas from Scarborough and Reed Bank Seamounts (Tu et al., 1992) are shown for reference.

3.2. Trace elements

As a group, the primitive high-K basalts from the central segment have the highest average content of compatible trace elements (e.g., Ni, Cr, Co, V), generally followed by the three magnesian basaltic samples from the northeastern segment. There is a systematic decrease in compatible trace elements from the primitive basalts to the more evolved lavas (Fig. 3), although the high-K calc-alkaline sample (P90-61) deviates strongly from this pattern. Surprisingly, the primitive basalts also have the highest incompatible trace element (e.g., Nb, Sr, Ba, Rb) contents and there is general decrease in the incompatible trace elements from basalts to basaltic andesites (Fig. 3). This is opposite to the predicted behavior of these elements with an increasing degree of magma differentiation (e.g. Shaw, 1970). The high-K basaltic andesite again

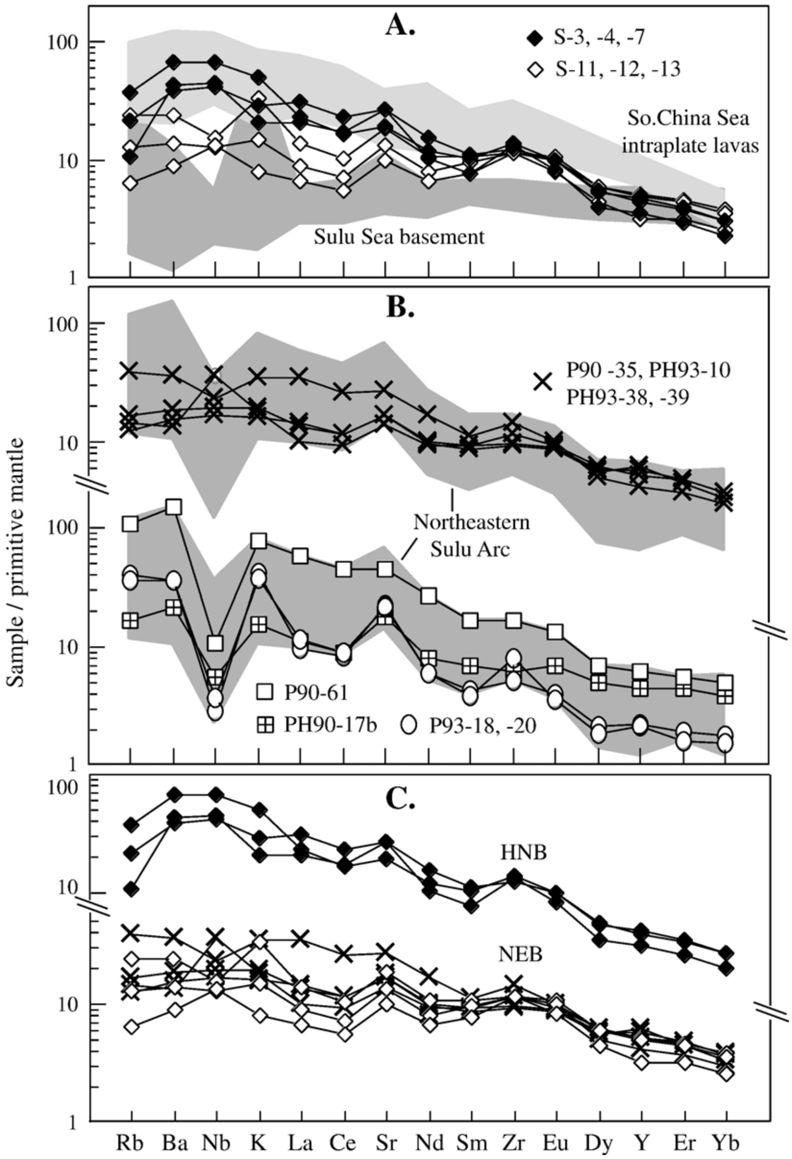

Fig. 4. Trace element diagrams, normalized to primitive mantle values of Sun and McDonough (1989), for the Sulu Arc samples. A. Representative central Sulu Arc lavas are shown relative to the most enriched Scarborough and Reed Bank Seamount lavas from South China Sea (Tu et al., 1992) and depleted Sulu Sea igneous basement lavas (Spadea et al., 1996). B. Representative northeastern Sulu Arc lavas relative to the full set for the northeastern segment lavas (Sajona et al., 1993, 1996). Samples P90-35, PH93-38, PH93-39, and PH93-10 have slight negative to positive Nb anomalies whereas PH90-17B, PH93-18, P90-20, and P90-61 have distinct negative Nb anomalies. C. Representative HNB and NEB from the central and northeastern segments of the Sulu Arc.

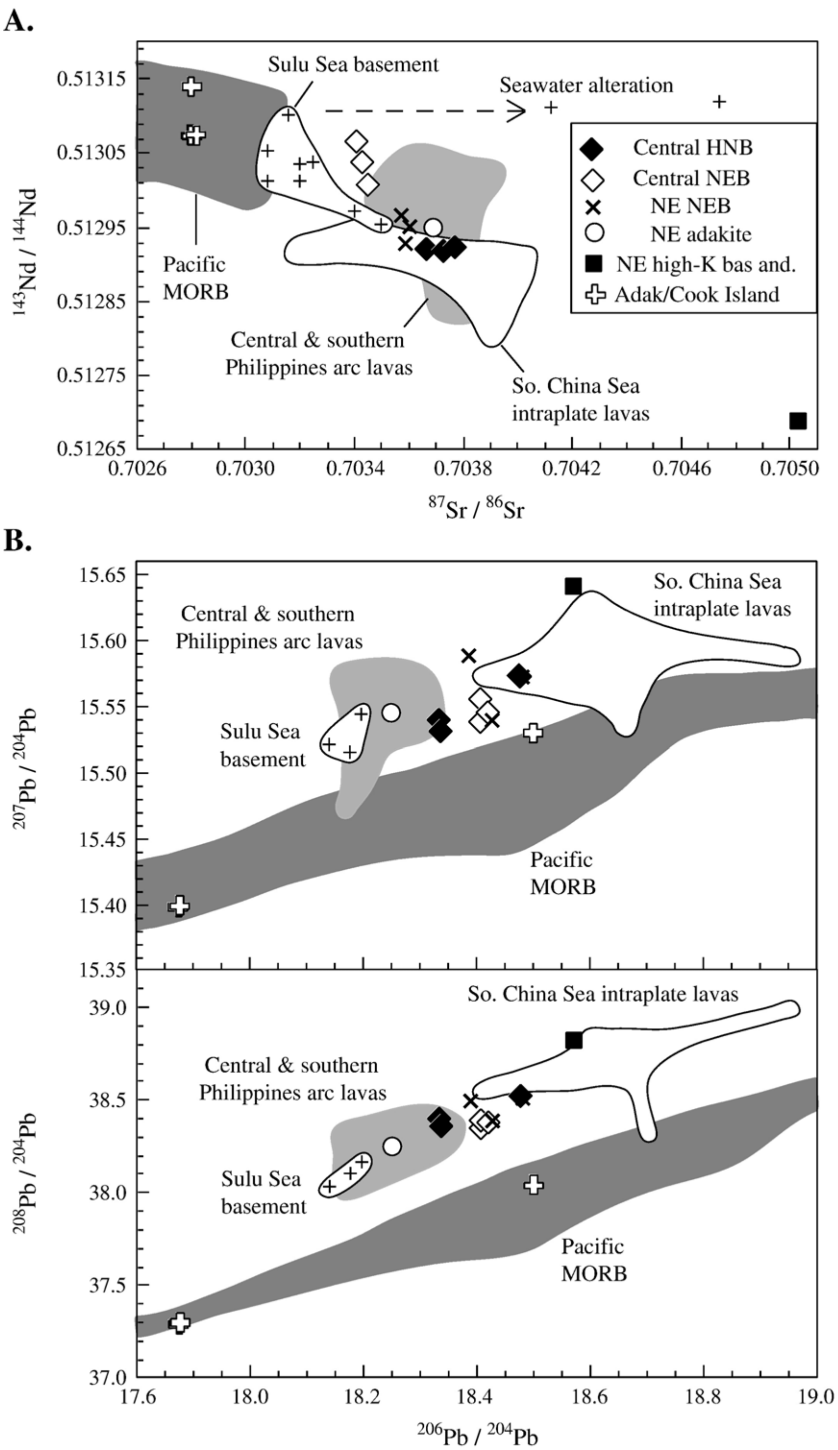

Fig. 5. A. Sr versus Nd isotopic data for Sulu samples, as well as for South China Sea intraplate lavas (Tu et al., 1992), Sulu Sea igneous basement (Spadea et al., 1996) and representative slab melts (Yogodzinski et al., 1995; Stern and Killian, 1996). Southern Philippines arc lava field based on data from Castillo et al. (1999) and Sajona et al. (2000). B. Pb isotopic variation diagrams for Sulu Arc lavas, South China Sea intraplate lavas (Tu et al., 1992), Sulu Sea basement lavas (Spadea et al., 1996), and representative slab melts (Yogodzinski et al., 1995; Stern and Killian, 1996). MORB field adapted from Ito et al. (1987).

deviates from the general trends and the two evolved adakites have higher incompatible trace element contents, save for Nb, than the rest of the northeastern segment lavas.

In detail, the trace element concentration patterns—particularly with regard to the HFSE—of the different sample groups exhibit significant differences. Unlike typical arc volcanic rocks, the absolute Nb contents in the central segment primitive basalts range from 30 to 48 ppm, therefore placing them in the category of HNB (cf. Reagan and Gill, 1989; Defant et al., 1992). These primitive basalts have positive Nb and Zr anomalies (Fig. 4A) and do not possess high LREE/HFSE ratios, with La/Nb ratios lower than typical island arc basalts (Fig. 4A; $La/Nb_{PM}=0.35$–0.74 versus >2, respectively; Perfit et al., 1980; Bailey et al., 1987; Kersting and Arculus, 1994); they also have low LILE/HFSE ratios (e.g., $Rb/Nb_{PM}=0.24$–0.56). The primitive basalts, however, have the greatest enrichment in LREE relative to HREE, with $La/Yb_{PM}=7.6$–10.0.

The northeastern segment magnesian basalts and basaltic andesites have lower overall contents of Nb (12–26 ppm) yet exhibit a range of Nb anomalies from positive to only weakly negative (Fig. 4B; $La/Nb_{PM}=0.3$–0.9; $Rb/Nb_{PM}=0.4$–0.9) falling into Sajona et al.'s (1996) classification of NEB. Their REE patterns have shallower slopes than the central segment primitive basalts, with $La/Yb_{PM}=2.8$–4.3. The high-K basaltic andesite (P90-61) has high Nb (7.7 ppm), but also has high LREE (39.7 ppm La) and LILE (68 ppm Rb) leading to typical arc trace element patterns, with a strong negative Nb anomaly ($La/Nb_{PM}=5.4$) and LREE-enriched pattern (Fig. 4B; $La/Yb_{PM}=11.7$).

Most of the andesites and dacites from the northeastern segment, which Sajona et al. (1996) classified as adakites, contrast sharply with the NEB and HNB in their trace element characteristics. They have high Sr/Y (>45) and low overall Y (<10 ppm) and HREE contents (e.g., <1 ppm Yb), which are close to the typical values of adakites (Sr/Y>40; Y<15–18 ppm; Yb<1–1.2 ppm) (e.g., Defant and Drummond, 1990; Peacock et al., 1994). They are marked by much lower HFSE contents (2–3 ppm Nb) and correspondingly larger LILE/HFSE ($Rb/Nb_{PM}>9$) and LREE/HFSE ($La/Nb_{PM}>3$) ratios, and strong negative Nb anomalies (Fig. 4B).

In summary, the samples analyzed in this study can be divided into distinct groups based on their incompatible trace element contents (Fig. 4A to C): (1) HNB (S-3, S-4, S-7, and S-8 from the central segment), (2) NEB (S-11, S-12 and S-14 from the central segment and P90-35, PH93-38 and PH93-39 from the northeastern segment), (3) adakites (PH93-18 and P90-20), (4) high-K basaltic andesite (P90-61) and (5) low-K basaltic andesite (PH90-17B). Sample PH93-10 from the northeastern segment is also classified as NEB despite its HNB-like trace element concentration pattern because of it has low Nb content (16 ppm) and is relatively differentiated ($SiO_2=55\%$ and $MgO=5\%$).

3.3. Isotopes

There is considerable variation in Sr and Nd isotopic ratios among the Sulu Arc samples (Table 1, Fig. 5A). Values of $^{87}Sr/^{86}Sr$ range from 0.70360 to 0.70377 for the HNB and overlap with the NEB from the northeastern segment ($^{87}Sr/^{86}Sr=0.70360$), but not with the NEB from the central segments ($^{87}Sr/^{86}Sr=0.70341$–0.70345). The analyzed adakite ($^{87}Sr/^{86}Sr=0.70369$) falls within the HNB range, whereas the high-K basaltic andesite (P90-61) has the highest $^{87}Sr/^{86}Sr$ ratio (0.70504) among the samples. Ratios of $^{143}Nd/^{144}Nd$ of the HNB are fairly uniform (~0.51292) and on average are lower than the NEB and adakite ($^{143}Nd/^{144}Nd=0.51293$–$0.51307$). Again, the high-K calc-alkaline basaltic andesite has an extreme isotopic value, with a $^{143}Nd/^{144}Nd$ ratio of 0.51269. Most of the Sulu Arc Sr and Nd isotope values fall within the range of published values from other southern Philippines arc lavas and overlap with the intraplate lavas from the South China Sea (Fig. 5A; Tu et al., 1992; Castillo, 1996; Castillo et al., 1999; Sajona et al., 2000).

The Pb isotopic ratios of Sulu Arc lavas also show considerable range, but show more complexity than the Sr and Nd isotopic ratios (Table 1, Fig. 5B). As a whole, the Pb isotopic signature of the lavas overlaps with those of the more radiogenic South China Sea intraplate lavas and less radiogenic central and southern Philippines arc lavas (Fig. 5B; Tu et al., 1992; Castillo, 1996; Castillo et al., 1999; Sajona et al., 2000). The HNB are slightly more heterogeneous (e.g., $^{206}Pb/^{204}Pb=18.34$–18.48) than the NEB ($^{206}Pb/^{204}Pb=18.44$–18.48). As with the Sr and Nd isotopes, the high-K basaltic andesite has the most extreme Pb isotope ratios (e.g., $^{206}Pb/^{204}Pb=18.57$) among the samples; the adakite has the lowest $^{206}Pb/^{204}Pb$ (18.25) and $^{208}Pb/^{204}Pb$ (38.24) values.

4. Discussion

4.1. The origin of Sulu Arc adakites

Most of the andesites and dacites comprising the adakites in the northeastern segment have been proposed as products of partial melting of the subducted Sulu Sea crust (Sajona et al., 1996, 1994, 1993).

Andesites and dacites with similar compositional characteristics, however, have been found interbedded with basalts and basaltic andesites in other areas in southern and central Philippines; these high-silica lavas have been shown to originate from the contemporaneously erupted, more primitive basalts and basaltic andesites through fractional crystallization involving amphibole (+/− apatite) and magma mixing processes (e.g., Castillo et al., 1999; Solidum et al., 2003). Admittedly, the latter studies did not directly investigate the adakites from the northeastern Sulu Arc, but our new Sr and Nd isotopic data for one of these Sulu Arc adakites are indistinguishable from those of the basalts and basaltic andesites (excluding the high-K basaltic andesite; Fig. 5A). In turn, the northeastern Sulu Arc lavas are isotopically different from adakites from Adak and Cook Islands, which have the most normal-MORB like isotopic ratios (Fig. 5A and B; Yogodzinski et al., 1995; Stern and Killian, 1996). Moreover, the isotopic signature of the northeastern segment adakite is different from that of the Sulu Sea basement, the purported source of slab-derived melt beneath the Sulu Arc (Figs. 4 and 5). Finally, the trace element signature of the adakites such as ratios of Nb/Ta (9 and 13) and Zr/Hf (30 and 42; Table 1) are relatively lower and higher than chondritic ratios, respectively; these are inconsistent with an eclogite source (e.g., David et al., 2000; Foley et al., 2002; Weyer et al., 2003; Schmidt et al., 2004; Xiong et al., 2005). As a whole, the geochemical data suggest that the source of the northeastern segment adakites is not very much different from the source of the arc basaltic lavas, and that source is not the Sulu Sea basement. Consequently, the presence of slab melts in northeastern Sulu Arc is highly unlikely. Thus the observed chemical differences between these high-silica lavas and basaltic lavas in the northeastern segment most likely result from complex magmatic differentiation processes (Castillo et al., 1999; Solidum et al., 2003) or alternatively, remelting of the Sulu magmatic arc crust (e.g., Yumul et al., 1999, 2000).

4.2. The origin of basalts and basaltic andesites enriched in Nb

Sulu Arc Nb-enriched lavas are divided into HNB and NEB that differ in their bulk major and trace element compositions, particularly in their Nb contents (up to 48 ppm for HNB and up to 26 ppm for NEB), and to date NEB have been found associated with HNB in the central segment and with adakites in the northeastern segment. Despite their differences, however, they form sub-parallel and overlapping trace element concentration patterns (Fig. 3), have overlapping Pb isotopic ratios (Fig. 4) and have similar trace element signatures, such as similar Nb/Ta (17 to 22) and Zr/Hf (40 to 53) ratios (Table 1). These data suggest that they were formed by similar magmatic differentiation processes and/or came from fairly similar sources. Below, we show that the chemical similarities and differences between HNB and NEB cannot be ascribed to the magmatic differentiation processes that commonly affect many arc lava suites—crustal assimilation and fractional crystallization (AFC; e.g., Gill, 1981; Ewart and Hawkesworth, 1987; Devine, 1995). Then we evaluate the genesis of these atypical Sulu Arc lavas enriched in Nb through the aforementioned competing models: metasomatism of the mantle wedge by slab-derived melts through amphibole stabilization and mixing between HFSE-enriched and geochemically depleted mantle sources.

4.2.1. Fractional crystallization and crustal assimilation

A crystal fractionation origin of NEB from the primitive HNB is inconsistent with their discontinuous trends on Harker diagrams (Fig. 3), the higher incompatible trace element concentrations of HNB than NEB (Fig. 3) and the crossing patterns of their moderately incompatible trace element contents (Fig. 4C). Strontium and Nd isotopic data also do not support a simple crystal fractionation relationship between the two groups as they form distinct, though almost overlapping fields (Fig. 5A). Note that the HNB and NEB Pb isotopic ratios overlap, but we suspect that the Pb isotopic ratios cannot always be used as a conclusive argument for either case because the Pb isotopic signature of arc lavas can be severely compromised by the elemental mobility of Pb in subduction zone environment (e.g., Brenan et al., 1995; You et al., 1996).

There is a dearth of geochemical data for the Pre-Tertiary granitic rocks, metamorphic rocks, melanges, and slivers of variably metamorphosed ophiolitic blocks and associated sedimentary rocks that comprise the basement complex in the arc (Sajona et al., 1996). The few available geochemical data for metamorphic rocks in the basement complex in the northeastern segment, however, show characteristic depletion in HFSE and depletion to only mild-enrichment in other highly incompatible trace elements (Tamayo et al., 2000). Moreover, an amphibolite member of the basement complex in central Mindanao has a high Nd isotopic ratio ($^{143}Nd/^{144}Nd=0.51320$; P. Castillo, unpub. data), indicating a long time-integrated history of depletion in incompatible trace elements. Thus the few available data suggest that basement assimilation cannot produce the incompatible trace element enrichment in both NEB and HNB. Most importantly, the central segment sits on a thinner and perhaps entirely oceanic crust and the HNB are primitive lavas that are least likely affected by contamination by the basement complex. Yet the HNB have the greatest enrichment in Nb and other incompatible trace elements as well as lower Nd isotopic ratio.

4.2.2. Slab-derived melt metasomatism of the mantle wedge

The model that Sajona et al. (1993, 1994, 1996) proposed for the genesis of NEB in the Sulu Arc calls for melt derived from the subducted Sulu Sea crust to form amphibole enriched in HFSE in the mantle wedge. Convection of the mantle wedge then carries the amphibole to depths where it breaks down, releasing HFSE to the mantle source of NEB (see also, Kepezhinskas et al., 1996; Defant and Kepezhinskas, 2001). Thus, although NEB are not thought to be a direct product of slab-derived melt—reflected in the geochemical characteristics of NEB—in this model such a melt does play a crucial role in generating HFSE-enriched arc lavas.

As discussed earlier, lavas representing slab melts are most likely not present in northeastern Sulu Arc. However, it is by no means a proof that the subducted Sulu Sea basement does not melt beneath the arc and that such a melt directly or indirectly does not cause the HFSE enrichment in the mantle source or sources of HNB and NEB. What is important is to use available geochemical data to trace the enrichment of Nb in NEB and particularly in HNB, which have the highest absolute Nb concentrations and strongest positive Nb anomalies (Figs. 3 and 4). The HNB have consistently higher $^{87}Sr/^{86}Sr$ and lower $^{143}Nd/^{144}Nd$ ratios than the central segment NEB, and than the northeastern segment NEB to a limited extent. They have higher $^{87}Sr/^{86}Sr$ and lower $^{143}Nd/^{144}Nd$ ratios than the Sulu Sea basement lavas and adakites from Adak and Cook Islands, but overlap with those of the South China Sea intraplate lavas from Scarborough and Reed Bank Seamounts (Fig. 5A). On the other hand, the NEB, which have lower absolute Nb concentrations and weaker positive Nb anomalies than HNB, have Sr and Nd isotopic ratios that fall roughly between HNB and Sulu Sea basement (Fig. 5A). The Pb isotopic compositions of both HNB and NEB are distinct from that of the Sulu Sea basement (Fig. 5B).

The systematic Sr and Nd isotopic variation of the HNB, NEB and Sulu Sea basement lavas is difficult to reconcile with metasomatism of the mantle wedge by slab-derived melts. The metasomatism would require the formation in the mantle wedge of Nb-rich amphibole with low $^{143}Nd/^{144}Nd$ and high $^{87}Sr/^{86}Sr$ ratios by an adakite melt derived from the Sulu Sea basement with high $^{143}Nd/^{144}Nd$ and low $^{87}Sr/^{86}Sr$ values. Although it is possible to increase the $^{87}Sr/^{86}Sr$ ratio in the amphibole through an extremely high Rb/Sr during the short time span from the early–middle Miocene slab subduction to Pliocene–Pleistocene lava eruption, this is inconsistent with the observed Rb and Sr contents in the HNB and NEB (Table 1). Most importantly, lowering the $^{143}Nd/^{144}Nd$ ratio in the amphibole poses a huge dilemma. As implied earlier, changing the isotopic composition of the primitive HNB through assimilation of the basement complex in the central Sulu Arc is also highly unlikely. Thus the most likely interpretation for the Sr and Nd isotopic data is that the source or sources of HNB and NEB is/are not the Sulu Sea basement or its source, but is/are more similar to that of the South China Sea intraplate lavas.

The concentrations of HFSE in the Sulu Arc lavas also do not offer support for the adakite metasomatism model. For both the HNB and NEB, Nb exhibits positive correlation with some of the incompatible trace elements (e.g., Rb, Ba, Zr, Ta), with the HNB again trending towards South China Sea intraplate lavas and the NEB going towards the Sulu Sea basement (Fig. 6; see also, Castillo et al., 2002). Kepezhinskas et al. (1996) had presumed that such correlation represents a product of metasomatism of the mantle wedge by both HFSE-enriched amphibole and hydrous subduction component, but this explanation is equivocal. Moreover, the breakdown of amphibole in such a metasomatized mantle wedge is more likely to produce the high magnesian andesites commonly found in volcanic arcs, as reflected in melting experiments on hydrous upper mantle (e.g., Kushiro, 1974; Tatsumi, 1981), rather than the rare HNB (Castillo et al., 2002).

The Nb/Ta (17 to 23) and Zr/Sm (27 to 43) ratios of HNB and NEB from the central segment (Table 1) greatly overlap with those of OIB (17.8 and 35.9, respectively) and normal-MORB (17.7 and 36.1, respectively; Sun and McDonough, 1989). Their Zr/Hf ratios (40 to 51) also overlap with OIB and normal-MORB values, which range from 35 to 44 (David et al., 2000). The Nb/Ta and Zr/Sm ratios are inconsistent with an amphibolite or eclogite source for HNB and NEB (e.g., Foley et al., 2002; Schmidt et al., 2004; Xiong et al., 2005), but consistent with a sub-oceanic mantle source. The Nb/Ta (2–21) and Zr/Sm (23–33) ratios of the northeastern segment NEB are on average lower than those of HNB and the central segment NEB. These low ratios overlap with typical island arc basalts (Foley et al., 2002).

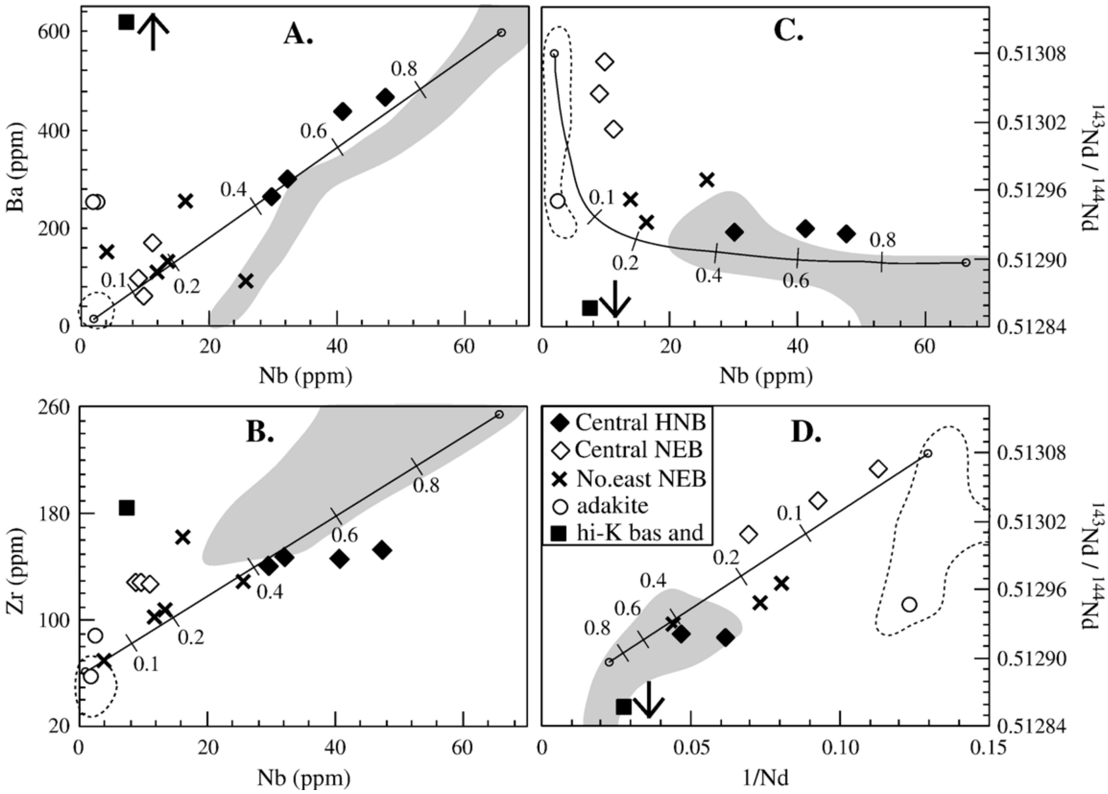

Fig. 6. A) Nb versus Ba, B) Nb versus Zr, C) Nb versus $^{143}Nd/^{144}Nd$, and D) $^{143}Nd/^{144}Nd$ versus 1/Nd diagrams for Sulu Arc lavas. Shown for reference are model curves generated through mixing (Langmuir et al., 1978; Faure, 1986) between a depleted (a Sulu Sea basement basalt with 2 ppm Nb, 8 ppm Ba, 65 ppm Zr; Spadea et al., 1996) and an enriched mantle end-component (a South China Sea seamount basalt containing 66 ppm Nb, 600 ppm Ba, 253 ppm Zr; Tu et al., 1992). Tick marks in the curves represent the amount of enriched component in the mixture.

Finally, it has been proposed that the HFSE, which are resistant to alteration and low-grade metamorphism, can be used as tectonic indicators (e.g., Pearce and Cann, 1973; Meschede, 1986). Fig. 7 is one of the diagrams commonly used for this purpose and indeed, it successfully discriminates the modern Sulu Sea basement and Scarborough and Reed Bank intraplate lavas into their respective plate boundary (normal-MORB or volcanic arc basalt association) and within-plate (alkalic or tholeiitic basalt association to plume-type MORB association) tectonic settings. It also assigns the typical, HFSE-depleted Sulu Arc lavas from the northeastern segment (Sajona et al., 1996) rightfully in the volcanic arc basalt association. Interestingly, it assigns HNB together with the Scarborough and Reed Bank intraplate lavas, almost exclusively in the within-plate alkalic basalt association, and NEB between HNB and typical Sulu Arc lavas. Thus the HFSE, combined with other incompatible trace elements and isotopic ratios of Sulu Arc lavas, simply suggest that the source of HNB is not the Sulu Sea basement or its source, but instead is the compositionally heterogeneous mantle source of the South China Sea intraplate lavas.

4.2.3. Mantle heterogeneity and mixing

The general positive correlation between Nb and other incompatible trace elements, particularly when viewed alongside the distinct Sr and Nd isotopic and other trace element differences among the HNB, NEB, subducting Sulu Sea basement, and South China Sea intraplate lavas suggests a simple binary mixture of mantle source components (Castillo et al., 2002). In this model, the varying enrichment in Nb and other HFSE among the Nb-enriched Sulu Arc lavas results from different degrees of mixing between two source components—a depleted one with MORB-like HFSE and other incompatible trace element concentrations and an enriched one possessing OIB-like trace element characteristics. This mixing model suggests that the magma source beneath the Sulu Arc, similar to that beneath the Sulu and South China Sea Basin, is a “marble cake” type or veined mantle, with enriched

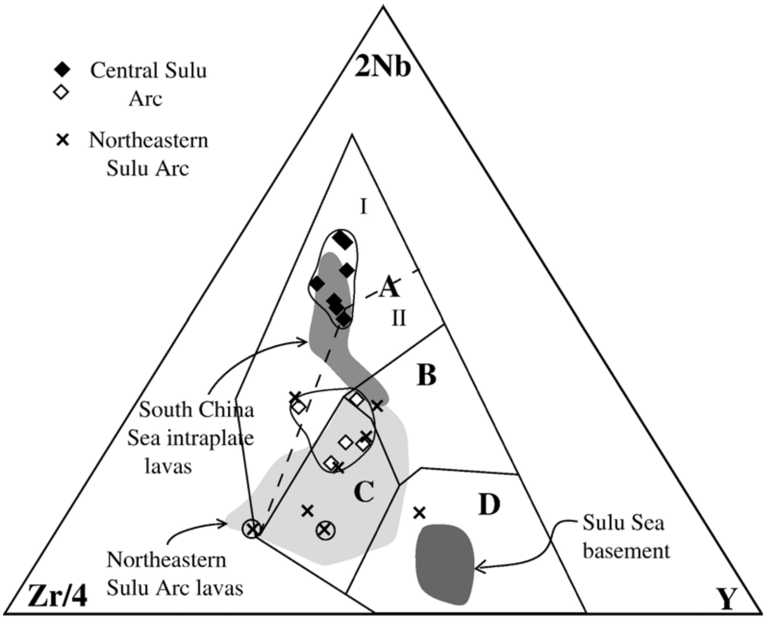

Fig. 7. Nb–Zr–Y triangular diagram commonly used to discriminate basaltic lavas from different tectonic settings (after Meschede, 1986). Field AI represents within-plate alkali basalts; AII within-plate alkali and tholeiitic basalts; B plume-type mid-ocean ridge basalts; C within-plate tholeiitic and volcanic arc basalts; and D volcanic arc and normal mid-ocean ridge basalts. Note that majority of the Central Sulu Arc primitive basalts plot in the within-plate alkali basalt field, majority of the Central Sulu Arc basaltic andesites and northeastern basalts and basaltic andesites plot in the within-plate tholeiitic and volcanic arc basalts fields. The two adakites are circled. Shown for reference are the South China Sea intraplate lavas (Tu et al., 1992), and northeastern Sulu Arc (Sajona et al., 1993, 1996) and Sulu Sea igneous basement (Spadea et al., 1996).

components of varying size embedded in a depleted matrix (Castillo et al., 2002; Hirschmann et al., 2003).

Simple linear mixing models can be constructed in the Nb versus incompatible trace element variation diagrams (Fig. 6A to C) using two mantle end-components represented by a typical depleted Sulu Sea crust (Spadea et al., 1996) and one of the enriched Reed Bank lavas (Tu et al., 1992). For the relationship Nb versus Ba and Zr, for example, calculation models indicate that the primitive central Sulu Arc HNB represent mixtures containing >40% to <80% of enriched component, compared to <10% to ~30% in the NEB. Calculations based on Nb versus $^{143}Nd/^{144}Nd$ and 1/Nd versus $^{143}Nd/^{144}Nd$ ratios (Fig. 6D), however, suggest more variable mixtures, ranging from >30% to <80% of enriched component in the HNB and $\ll$10% to ~40% in the NEB. The scatter along the mixing lines in these diagrams of the HNB and NEB can be explained as reflecting heterogeneity within both the enriched and depleted components, such as differing sizes and/or degrees of enrichment of the enriched end-component and particularly by the variable degrees of metasomatism or fluxing of the depleted end-component with subduction component. Scattering of data along the mixing line is also expected because individual batches of HNB and NEB magmas expelled from the mantle must have been affected by other fractionation processes on their way to the crust. For example, the northeastern NEB, which were erupted in a thicker and chemically more complex arc crust, show relatively more trace element variation than central NEB and this is most probably due to crustal contamination. Note that the model is for the generation of HNB and NEB only, and does not pertain to the generation of HFSE-depleted basalts, basaltic andesites, andesites, and adakites from the northeastern segment of the Sulu Arc. The parental magmas that gave rise to this typical arc lava suite most probably originated from the depleted mantle wedge metasomatized by the subduction component.

Our proposed mixing of enriched and depleted mantle components differs from that suggested by Reagan and Gill (1989) to explain the origin of HNB from the Central American convergent margin. In their model, small-degree melts, undersaturated in rutile, are mixed with high-degree melts possessing MORB-like trace element characteristics. Undersaturation of rutile is maintained by low oxygen fugacities in the sub-arc mantle, caused by the migration of C–O–H volatiles (primarily CH_4) within small-degree melts from the asthenosphere into the mantle wedge, either through or around the edge of a young subducting slab (Reagan and Gill, 1989). This mechanism can explain the observed association of NEB and HNB with the subduction of young and/or hot oceanic lithosphere (e.g. Leeman et al., 1990; Defant et al., 1992; Defant and Drummond, 1993; Kepezhinskas et al., 1996; Sajona et al., 1996; Aguillón-Robles et al., 2001), as well as the co-occurrence in some arcs (as at Zamboanga) of HFSE-enriched lavas and calc-alkaline basalts, but is inconsistent with the systematic Sr and Nd isotopic variation among these lavas.

The origin of HNB and NEB through mixing of components within a heterogeneous mantle is similar to the process proposed by Wallace and Carmichael (1999). They attributed the heterogeneity of convergent margin magmas from central Mexico to convection in the mantle wedge, bringing back-arc asthenosphere under the volcanic front, with HFSE variability arising from possible pre-convection heterogeneity and/or overprinting by previous melt extraction and/or fluids derived from the subducting slab. Pilet et al. (2004) additionally have proposed that intraplate magmatism can create, through percolative fractional crystallization, veins containing Nb-rich oxides within the upper mantle. In our proposed scenario, mantle heterogeneity is clearly exhibited by intraplate magmatism in the Sulu Sea Basin. Either such Nb-rich oxides or outright-enriched mantle components were trapped beneath the nascent Sulu Arc in the middle Miocene. Melting of isolated pockets of such enriched mantle components occurs in relatively cold, intraplate setting away from spreading ridges (e.g., Batiza and Vanko, 1984; Tu et al., 1992), and thus we envision that they can also melt in the relatively cold, subduction zone environment.

5. Summary and conclusion

Some of the basalts and basaltic andesites in the central and northeastern segments of the Sulu Arc are either HNB or NEB. Geochemical similarities within—as well as between—the two lava groups suggest that a similar process, or set of processes, is responsible for their departure from the typical HFSE-depleted signature of convergent margin lavas.

The trace element and Sr and Nd isotopic data for the Sulu Arc samples are consistent with a model in which the HNB and NEB are simply the products of variable degrees of mixing between geochemically depleted and geochemically enriched, easily meltable mantle sources. The presence of enriched intraplate lavas in the nearby South China Sea Basin (i.e., Reed Bank and Scarborough Seamount lavas) is consistent with the presence of a compositionally heterogeneous mantle in the region with regard to the HFSE and other incompatible trace elements and isotopic data. The differing degrees of enrichment between and within the Sulu HNB and NEB can be seen as reflecting varying additions of the enriched component (e.g., >30 to <80% for the HNB and <10% to ~40% for the NEB) to a depleted component, suggesting that in addition to the flux of subduction component, the mantle wedge beneath the Sulu Arc consists of enriched veins or regions of varied size within a depleted matrix. The possible influence of back-arc and mantle wedge convection processes—including previous melt extraction and percolative fractional crystallization—further highlights the role HNB and NEB can play in studying the cycling of HFSE and other elements within a broader global context, and suggests the presence of HNB and NEB in volcanic arcs is not an unambiguous signal of slab melting and/or caution is needed when using HFSE enrichment as a tracer for mantle metasomatism by slab melt.

Acknowledgements

We thank C. MacIsaac and K. Walda for their help in the geochemical analyses, D. Sajona for providing some of the samples, T. Horscroft for editorial handling, and S. Foley and two anonymous reviewers for their constructive comments that greatly improved the manuscript. Portions of the manuscript are parts of the M.Sc. dissertation of S.J.R. This work was supported by NSF-EAR00-01212 and is dedicated to the late R.S. Punongbayan, our beloved mentor and friend.

References

Aguillón-Robles, A., Calmus, T., Benoit, M., Bellon, H., Maury, R.C., Cotten, J., Bourgois, J., Michaud, F., 2001. Late Miocene adakites and Nb-enriched basalts from Vizcaino Peninsula, Mexico: indicators of East Pacific Rise subduction below southern Baja California? Geology 29, 531–534.

Apuada, N.A., Camit, R.A., Clemente, V.C., Pagado, E.S., 1992. Resource Assessment of the Mt. Ampiro Geothermal Prospect, Misamis Occidental, Mindanao, Philippines. PNOC-EDC, Manila.

Bailey, J.C., Frolova, T.I., Burikova, I.A., 1987. Mineralogy, geochemistry and petrogenesis of Kurile island-arc basalts. Contributions to Mineralogy and Petrology 102, 265–280.

Batiza, R., Vanko, R., 1984. Petrology of young Pacific seamounts. Journal of Geophysical Research 89, 11,235–11,260.

Brenan, J.M., Shaw, H.F., Phinney, D.L., Ryerson, F.J., 1994. Rutile-aqueous fluid partitioning of Nb, Ta, Hf, Zr, U and Th: implications for high field strength element depletions in island-arc basalts. Earth and Planetary Science Letters 128, 327–339.

Brenan, J.M., Shaw, H.F., Ryerson, F.J., 1995. Experimental evidence for the origin of lead enrichment in convergent-margin magmas. Nature 378, 54–56.

Castillo, P.R., 1996. The origin and geodynamic implication of the Dupal isotopic anomaly in volcanic rocks from the Philippine island arcs. Geology 24, 271–274.

Castillo, P.R., Newhall, C.G., 2004. Geochemical constraints on possible subduction components in lavas of Mayon and Taal

Volcanoes, southern Luzon, Philippines. Journal of Petrology 43, 1089–1108.
Castillo, P.R., Janney, P.E., Solidum, R., 1999. Petrology and geochemistry of Camiguin Island, southern Philippines: insights into the source of adakite and other lavas in a complex arc tectonic setting. Contributions to Mineralogy and Petrology 134, 33–51.
Castillo, P.R., Solidum, R.U., Punongbayan, R.S., 2002. Origin of high field strength element enrichment in the Sulu Arc, southern Philippines, revisited. Geology 30, 707–710.
David, K., Schiano, P., Allègre, C.J., 2000. Assessment of the Zr/Hf fractionation in oceanic basalts and continental materials during petrogenetic processes. Earth and Planetary Science Letters 178, 285–301.
Defant, M.J., Drummond, M.S., 1990. Derivation of some modern arc magmas by melting of young subducted lithosphere. Nature 347, 662–665.
Defant, M.J., Drummond, M.S., 1993. Mount St. Helens: potential example of the partial melting of the subducted lithosphere in a volcanic arc. Geology 21, 541–550.
Defant, M.J., Kepezhinskas, P., 2001. Evidence suggests slab melting in arc magmas. Eos, Transactions of the American Geophysical Union 82, 67–70.
Defant, M.J., Richerson, M., de Boer, J.Z., Stewart, R.H., Maury, R.C., Bellon, H., Drummond, M.S., Feigenson, M.D., Jackson, T.E., 1991. Dacite genesis via both slab melting and differentiation: petrogenesis of La Yeguada volcanic complex, Panama. Journal of Petrology 32, 1101–1142.
Defant, M.J., Jackson, T.E., Drummond, M.S., de Boer, J.Z., Bellon, H., Feigenson, M.D., Maury, R.C., Stewart, R.H., 1992. The geochemistry of young volcanism throughout western Panama and southeastern Costa Rica: an overview. Journal of the Geological Society (London) 149, 569–579.
Devine, J.D., 1995. Petrogenesis of the basalt–andesite–dacite association of the Grenada Lesser Antilles island arc, revisited. Journal of Volcanology and Geothermal Research 69, 1–33.
Elliot, T., Plank, T., Zindler, A., White, W., Bourdon, B., 1997. Element transport from slab to volcanic front at the Mariana arc. Journal of Geophysical Research 102, 14991–15019.
Ewart, A., Hawkesworth, C.J., 1987. The Pleistocene–Recent Tonga–Kermadec arc lavas: interpretation of new isotopic and rare earth data in terms of a depleted mantle source model. Journal of Petrology 28, 495–530.
Faure, G., 1986. Principles of Isotope Geology. John Wiley and Sons, New York. 589 pp.
Foley, S., Tiepolo, M., Vannucci, R., 2002. Growth of early continental crust controlled by melting of amphibolite in subduction zones. Nature 417, 837–840.
Gamble, J.A., Smith, I.E.M., McCulloch, M.T., Graham, I.J., Kokelaar, B.P., 1993. The geochemistry and petrogenesis of basalts from the Taupo volcanic zone and Kermadec island arc, S.W. Pacific. Journal of Volcanology and Geothermal Research 54, 265–290.
Gill, J.B., 1981. Orogenic Andesites and Plate Tectonics. Springer-Verlag, Berlin. 358 pp.
Govindaraju, K., 1989. 1989 compilation of working values and sample descriptions for 272 geostandards. Geostandards Newsletter 13, 1–113.
Green, T.H., Pearson, N.J., 1986. Ti-rich accessory phase saturation in hydrous mafic–felsic compositions at high P, T. Chemical Geology 54, 185–201.
Hamilton, W., 1979. Tectonics of the Indonesian Region. USGS Professional Paper 1078.
Hawkesworth, C.J., Hergt, J.M., Ellam, R.M., McDermott, F., 1991. Element fluxes associated with subduction related magmatism. Philosophical Transactions of the Royal Society of London 335, 393–405.
Hawkesworth, C.J., Gallagher, K., Hergt, J.M., McDermott, F., 1993. Mantle and slab contributions in arc magmas. Annual Review of Earth and Planetary Sciences 21, 175–204.
Hinz, K., Block, M., 1990. Summary of geophysical data from the Sulu and Celebes Seas. In: Rangin, C., Silver, E. (Eds.), Proceedings, Ocean Drilling Program Initial Reports, vol. 124. Ocean Drilling Program, College Station, TX, pp. 87–92.
Hirschmann, M.M., Kogiso, T., Baker, M.B., Stolper, E.M., 2003. Alkalic magmas generated by partial melting of garnet pyroxenite. Geology 31, 481–484.
Hollings, P., 2002. Archean Nb-enriched basalts in the northern Superior Province. Lithos 64, 1–14.
Ito, E., White, W.M., Göpel, C., 1987. The O, Sr, Nd and Pb isotope geochemistry of MORB. Chemical Geology 62, 157–176.
Janney, P.E., Castillo, P.R., 1996. Basalts from the Central Pacific Basin: evidence for the origin of Cretaceous igneous complexes in the Jurassic Western Pacific. Journal of Geophysical Research 101, 2875–2894.
Kelemen, P.B., Johnson, K.T.M., Kinzler, R.J., Irving, A.J., 1990. High-field-strength element depletions in arc basalts due to mantle–magma interaction. Nature 345, 521–524.
Kelemen, P.B., Shimizu, N., Dunn, T., 1993. Relative depletion of niobium in some arc magmas and the continental crust: partitioning of K, Nb, La and Ce during melt/rock reaction in the upper mantle. Earth and Planetary Science Letters 120, 111–133.
Kepezhinskas, P.K., Defant, M.J., Drummond, M.S., 1996. Progressive enhancement of island arc mantle by melt–peridotite interaction inferred from Kamchatka adakites. Geochimica et Cosmochimica Acta 60, 1217–1229.
Kersting, A.B., Arculus, R.J., 1994. Klyuchevskoy Volcano, Kamchatka, Russia: the role of high-flux recharged, tapped and fractionated magma chamber(s) in the genesis of high-Al_2O_3 from high-MgO basalt. Journal of Petrology 35, 1–41.
Kushiro, I., 1974. Melting of hydrous upper mantle and possible generation of andesite magma: an approach from synthetic systems. Earth and Planetary Science Letters 22, 294–299.
Langmuir, C.H., Vocke Jr., R.D., Hanson, G.N., Hart, S.R., 1978. A general mixing equation with application to Icelandic basalts. Earth and Planetary Science Letters 37, 380–392.
Leeman, W.P., Smith, D.R., Hildreth, W., Palacz, Z., Rogers, N., 1990. Compositional diversity of Late Cenozoic basalts in a transect across the Southern Washington Cascades: implications for subduction zone magmatism. Journal of Geophysical Research 95, 19561–19582.
Lugmair, G.W., Galer, S.J.G., 1992. Age and isotopic relationships among the angerites Lewis Cliff 86010 and Angra dos Reis. Geochimica et Cosmochimica Acta 56, 1673–1694.
Maury, R.C., Defant, M.J., Joron, J.-L., 1992. Metasomatism of the sub-arc mantle inferred from trace elements in Philippine xenoliths. Nature 360, 661–663.
McCulloch, M.T., Gamble, J.A., 1991. Geochemical and geodynamical constraints on subduction zone magmatism. Earth and Planetary Science Letters 102, 358–374.
Meschede, M., 1986. A method of discriminating between different types of mid-ocean ridge basalts and continental tholeiites with the Nb–Zr–Y diagram. Chemical Geology 56, 207–218.
Peacock, S.M., Rushmer, T., Thompson, A.B., 1994. Partial melting of subducting oceanic crust. Earth and Planetary Science Letters 121, 227–244.

Pearce, J.A., Cann, J.R., 1973. Tectonic setting of basic volcanic rocks determined using trace element analyses. Earth and Planetary Science Letters 19, 290–300.
Pearce, J.A., Peate, D.W., 1995. Tectonic implications of the composition of volcanic arc magmas. Annual Review of Earth and Planetary Sciences 23, 251–285.
Pearce, J.A., Kempton, P.D., Nowell, G.M., Noble, S.R., 1999. Hf–Nd element and isotope perspective on the nature and provenance of mantle and subduction components in western Pacific arc–basin systems. Journal of Petrology 40, 1579–1611.
Peccerillo, A., Taylor, S.R., 1976. Geochemistry of Eocene calc-alkaline volcanic rocks from the Kastamonu area, northern Turkey. Contributions to Mineralogy and Petrology 58, 63–81.
Perfit, M.R., Gust, D.A., Bence, A.E., Arculus, R.J., Taylor, S.R., 1980. Chemical characteristics of island arc basalts: implications for mantle sources. Chemical Geology 30, 227–256.
Pilet, S., Hernandez, J., Bussy, F., Sylvester, P.J., 2004. Short-term metasomatic control of Nb/Th ratios in the mantle sources of intraplate basalts. Geology 32, 113–116.
Pubellier, M., Quebral, R., Rangin, C., Deffontaines, B., Muller, C., Butterlin, J., Manzano, J., 1991. The Mindanao collision zone: a soft collision event within a continuous Neogene strike-slip setting. Journal of Southeast Asian Earth Sciences 6, 239–248.
Rangin, C., Silver, E.A., 1991. Neogene tectonic evolution of the Celebes–Sulu basins: new insights from Leg 124 drilling. In: Silver, E., Rangin, C. (Eds.), Proceedings, Ocean Drilling Program Scientific Results, vol. 124. Ocean Drilling Program, College Station, TX, pp. 51–64.
Reagan, M.K., Gill, J.B., 1989. Coexisting calkalkaline and high-niobium basalts from Turrialba volcano, Costa Rica: implications for residual titanites in arc magma sources. Journal of Geophysical Research 94, 4619–4633.
Roeser, H.A., 1991. Age of the crust of the southeast Sulu Sea basin based on magnetic anomalies and age determined at Site 768. In: Silver, E., Rangin, C. (Eds.), Proceedings, Ocean Drilling Program Scientific Results, vol. 124. Ocean Drilling Program, College Station, TX, pp. 339–344.
Sajona, F.G., Maury, R.C., Bellon, H., Cotten, J., Defant, M.J., Pubellier, M., 1993. Initiation of subduction and the generation of slab melts in western and eastern Mindanao, Philippines. Geology 21, 1007–1010.
Sajona, F.G., Bellon, H., Maury, R.C., Pubellier, M., Cotten, J., Rangin, C., 1994. Magmatic response to abrupt changes in tectonic setting: Pliocene–Quaternary calc-alkaline lavas and Nb-enriched basalts of Leyte and Mindanao (Philippines). Tectonophysics 237.
Sajona, F.G., Maury, R.C., Bellon, H., Cotten, J., Defant, M.J., 1996. High field strength element enrichment of Pliocene–Pleistocene island arc basalts, Zamboanga Peninsula, western Mindanao (Philippines). Journal of Petrology 37, 693–726.
Sajona, F.G., Maury, R.C., Pubellier, M., Leterrier, J., Bellon, H., Cotten, J., 2000. Magmatic source enrichment by slab-derived melts in a young post-collision setting, central Mindanao (Philippines). Lithos 54, 173–206.
Santos, F.R., Pamatian, P.P., 1995. The Geology of the Mt. Malindang Geothermal Prospect, Misamis Occidental. PNOC-EDC, Manila.
Schmidt, M.W., Dardon, A., Chazot, G., Vannucci, R., 2004. The dependence of Nb and Ta rutile-melt partitioning on melt composition and Nb/Ta fractionation during subduction processes. Earth and Planetary Science Letters 226, 415–432.
Shaw, D.M., 1970. Trace element fractionation during anatexis. Geochimica et Cosmochimica Acta 34, 237–243.
Solidum, R.U., Castillo, P.R., Hawkins, J.W., 2003. Geochemistry of lavas from Negros Arc, west central Philippines: insights into the contribution from the subducting slab. Geochemistry, Geophysics, Geosystems 4, 1–26.
Spadea, P., D'Antonio, M., Thirlwall, M.F., 1996. Source characteristics of the basement rocks from the Sulu and Celebes Basins (Western Pacific): chemical and isotopic evidence. Contributions to Mineralogy and Petrology 123, 159–176.
Stern, C.R., Killian, R., 1996. Role of subducted slab, mantle wedge and continental crust in the generation of adakites from the Andean Austral volcanic zone. Contributions to Mineralogy and Petrology 123, 263–281.
Sun, S.-S., McDonough, W.F., 1989. Chemical and isotopic systematics of oceanic basalts: implications for mantle composition and processes. In: Saunders, A.D., Norry, M.J. (Eds.), Magmatism in the Ocean Basin. Geological Society [London] Special Publication, vol. 42, pp. 313–345.
Tamayo, R.A., Yumul, G.P., Maury, R.C., Bellon, H., Cotten, J., Polve, M., Juteau, T., Querubin, C., 2000. Complex origin for the south-western Zamboangan metamorphic basement complex, western Mindanao, Philippines. The Island Arc 9, 638–652.
Tatsumi, Y., 1981. Melting experiments on a high magnesian andesite. Earth and Planetary Science Letters 54, 357–365.
Tatsumi, Y., Hamilton, D.L., Nesbitt, R.W., 1986. Chemical characteristics of fluid phase released from a subducted lithosphere and origin of arc lavas: evidence from high-pressure experiments and natural rocks. Journal of Volcanology and Geothermal Research 29, 293–309.
Todt, W., Cliff, R.A., Hanser, R., Hofmann, A.W., 1996. Evaluation of a 202Pb–205Pb double spike for high precision lead isotope analyses. In: Basu, A., Hart, S. (Eds.), Reading of the Isotopic Code. American Geophysical Union Geophysical Monographs, vol. 95, pp. 429–437.
Tu, K., Flower, M.F.J., Carlson, R.W., Xie, G., Chen, C.-Y., Zhang, M., 1992. Magmatism in the South China Basin 1. Isotopic and trace-element evidence for an endogenous Dupal mantle component. Chemical Geology 97, 47–62.
Wallace, P.J., Carmichael, I.S.E., 1999. Quaternary volcanism near the valley of Mexico: implications for subduction zone magmatism and the effects of crustal thickness variations on primitive magma compositions. Contributions to Mineralogy and Petrology 135, 291–314.
Weyer, S., Münker, C., Mezger, K., 2003. Nb/Ta, Zr/Hf and REE in the depleted mantle: implications for the differentiation history of the crust–mantle system. Earth and Planetary Science Letters 205, 309–324.
Woodhead, J., Eggins, S., Gamble, J., 1993. High field strength and transition element systematics in island and back-arc basin basalts: evidence for multi-phase extraction and a depleted mantle wedge. Earth and Planetary Science Letters 114, 491–504.
Wyman, D.A., Ayer, J.A., Devaney, J.R., 2000. Niobium-enriched basalts from the Wabigoon subprovince, Canada: evidence for adakitic metasomatism above an Archean subduction zone. Earth and Planetary Science Letters 179, 21–30.
Xiong, X.L., Adam, J., Green, T.H., 2005. Rutile stability and rutile/melt HFSE partitioning during partial melting of hydrous basalt: implications for TTG genesis. Chemical Geology 218, 339–359.
Yogodzinski, G.M., Kay, R.W., Volynets, O.N., Koloskov, A.V., Kay, S.M., 1995. Magnesian andesite in the western Aleutian Komandorsky region: implications for slab melting and processes in the mantle wedge. Geological Society of America Bulletin 107, 505–519.
You, C-F., Castillo, P.R., Gieskes, J.M., Chan, L.H., Spivack, A.J., 1996. Trace element behavior in hydrothermal experiments:

implications for fluid processes at shallow depths in subduction zones. Earth and Planetary Science Letters 140, 41–52.
Yumul Jr., G.P., Dimalanta, C.B., Faustino, D.V., de Jesus, J.V., 1999. Silicic arc volcanism and lower crust melting: an example from the central Luzon, Philippines. Journal of Geology 154, 13–14.
Yumul Jr., G.P., Dimalanta, C.B., Bellon, H., Faustino, D.V., de Hesus, J.V., Tamayo Jr., R., Jumawan, F.T., 2000. Adakitic lavas in the central Luzon back-arc region, Philippines: lower crust partial melting products? The Island Arc 9, 499–512.